Photomagnetic Semiconductors

DOI: 10.1002/anie.201408680

Photomagnetic Response in Highly Conductive Iron(II) Spin-Crossover Complexes with TCNQ Radicals**

*Hoa Phan, Shermane M. Benjamin, Eden Steven, James S. Brooks, and Michael Shatruk**

In memory of James S. Brooks

Abstract: *Co-crystallization of a cationic Fe^{II} complex with a partially charged $TCNQ^{\bullet\delta-}$ (7,7′,8,8′-tetracyanoquinodimethane) radical anion has afforded molecular materials that behave as narrow band-gap semiconductors, $[Fe(tpma)(xbim)](X)(TCNQ)_{1.5}\cdot DMF$ ($X = ClO_4^-$ or BF_4^-; tpma = tris(2-pyridylmethyl)amine, xbim = 1,1′-(α,α′-o-xylyl)-2,2′-bisimidazole). Remarkably, these complexes also exhibit temperature-and light-driven spin crossover at the Fe^{II} center, and are thus the first structurally defined magnetically bistable semiconductors assembled with the $TCNQ^{\bullet\delta-}$ radical anion. Transport measurements reveal the conductivity of 0.2 $S\,cm^{-1}$ at 300 K, with the low activation energy of 0.11 eV.*

The preparation of multifunctional molecule-based materials is a challenging endeavor that has been actively pursued over the last decade. The seminal work by Coronado et al.,[1] who described the co-crystallization of a ferromagnetic layer of oxalato-bridged metal ions with conducting stacks of organic radicals, has sparked extensive research efforts aimed at creating novel molecular architectures that embed different functional components. A number of other molecular materials that exhibit both conductivity and magnetic ordering have been reported over the last decade.[2] The central challenge in the preparation of such hybrids lies in the need to provide magnetic exchange pathways to achieve long-range magnetic correlations. This requirement necessitates the formation of extended frameworks of metal ions connected by linkers capable of mediating significant magnetic interactions. In the majority of cases, co-crystallization of such extended fragments with other functional parts of the structure poses problems in terms of both crystallization kinetics (the need to combat the fast precipitation of extended structures) and structural commensurability.[3]

[*] H. Phan, Prof. M. Shatruk
Department of Chemistry & Biochemistry
Florida State University
95 Chieftan Way, Tallahassee, FL 32306 (USA)
E-mail: shatruk@chem.fsu.edu
Homepage: http://www.chem.fsu.edu/~shatruk/
S. M. Benjamin, E. Steven, Prof. J. S. Brooks[+]
Department of Physics and National High Magnetic Field Laboratory, Florida State University
1800 E Paul Dirac Dr, Tallahassee, FL 32310 (USA)
[+] Deceased on September 27, 2014.

[**] This research was supported by the National Science Foundation grants CHE-0911109 to M.S. and DMR-1309146 to J.S.B.
Supporting information for this article is available on the WWW under http://dx.doi.org/10.1002/anie.201408680.

An alternative to the magnetic order–disorder systems is offered by molecular materials that do not require long-range magnetic interactions to achieve magnetic bistability. We imply here single-molecule magnets[4] and spin-crossover (SCO) structures,[5] both of which can be observed in finite molecular complexes. In particular, in SCO complexes the interconversion between the high-spin (HS) and low-spin (LS) electronic configurations of a transition-metal ion can be triggered by changes in temperature, pressure, or light irradiation.[6] In recent years, there have been a number of attempts at merging the SCO with other functional properties.[7] In particular, co-crystallization of Fe^{III} SCO cations with the radical anions $[M(dmit)_2]^-$ (M = Ni, Pd, Pt; dmit = 1,3-dithiole-2-thione-4,5-dithiolate) led to hybrid semiconducting SCO materials.[8] A compilation of currently known SCO semiconductors is provided in Table 1.

Table 1: Semiconducting spin-crossover materials.

Compound	$T_{1/2}$ [K][a]	σ [$S\,cm^{-1}$][b]
$[Fe^{II}(dppTTF)_2][Ni(mnt)_2]_2(BF_4)\cdot PhCN$[7c]	240	2.6×10^{-3}
$[Fe^{III}(qnal)_2][Pd(dmit)_2]_5\cdot$acetone[8d]	220	1.6×10^{-3}
$[Fe^{III}(sal_2\text{-trien})][Ni(dmit)_2]$[8a]	220/243	0.2
$[Fe^{III}(salEen)_2]_2([Ni(dmit)_2]_5\cdot 6\,CH_3CN$[8c]	220	0.12
$[Fe^{III}(salten)Mepepy][M(dmit)]_2\cdot CH_3CN$[8b]	>300	0.1
$[Fe^{III}(qsal)_2][Ni(dmit)_2]_3\cdot CH_3CN\cdot H_2O$[8e]	330	2.0

[a] The temperature at which the fractions of the HS and LS ions are equal (two values indicate a hysteretic transition). [b] The room-temperature conductivity.

About 90% of the known SCO compounds are represented by complexes of the d^6 Fe^{II} ion.[5a] The spin transitions in the Fe^{II} complexes are, in general, more abrupt than in the complexes of other SCO ions. Until now, however, there have been only a few examples of the combination of Fe^{II} SCO complexes with organic radicals that could lead to the (semi)conducting SCO materials.[7b,c] Moreover, the combination of SCO complexes with TCNQ, one of the ubiquitous radicals in the preparation of synthetic conductors, has been essentially unexplored. The only structurally characterized example reported to date is an Fe^{II} SCO complex containing $TCNQ^-$ co-ligands,[9] but its conducting properties were not reported. Besides, to achieve significant charge transport in organic conductors, the radicals should carry a non-integer charge.[10] Herein, we report a simple approach to the synthesis of Fe^{II} complexes with partially charged $TCNQ^{\bullet\delta-}$ counterions. As will be shown below, these materials exhibit

both thermal- and light-induced SCO and high electrical conductivity.

We have recently reported that a combination of tetradentate tpma with *N*-alkylated 2,2′-bisimidazole derivatives offers a convenient ligand set for the preparation of robust SCO complexes.[11] In the present work, we combined the SCO cation, $[Fe(tpma)(xbim)]^{2+}$, with the organic radical anion, $TCNQ^{\bullet\delta-}$ ($\delta < 1$). To achieve the mixed valence of TCNQ, we used comproportionation reactions between its neutral and singly reduced forms in the presence of $[Fe(tpma)(xbim)]^{2+}$. These reactions led to the isolation of two crystalline complexes, $[Fe(tpma)(xbim)](X)(TCNQ)_{1.5}\cdot DMF$ ($X = ClO_4^-$ (**1**), BF_4^- (**2**)).

The crystal structures of **1** and **2** were determined at 230 and 100 K.[19] Both compounds crystallize in the *C*2/*c* space group. The asymmetric unit includes one $[Fe(tpma)(xbim)]^{2+}$ cation, one ClO_4^- or BF_4^- anion, one and a half partially charged $TCNQ^{\bullet\delta-}$ radicals, and one DMF solvent molecule (Figure 1). The crystal packing shows a clear separation of the structure into the cationic and anionic layers (Figure 2). The latter are composed of π-stacks of $TCNQ^{\bullet\delta-}$ radicals that propagate along the crystallographic *b* axis. The average Fe–N bond length in **1** decreases from 2.183 Å at 230 K to 2.057 Å at 100 K. These values are in the range typical of the HS and LS Fe^{II} complexes, respectively. The changes observed in the metal–ligand distances suggest the occurrence of temperature-induced SCO in complex **1**. Similar structural changes are observed for **2** (Table 2).

Table 2: Average Fe–N bond lengths and unit cell volumes (V_{UC}) and charges δ on crystallographically independent TCNQ molecules, A and B, in crystal structures of **1** and **2** determined at 100 K and 230 K.

Structural parameter	**1**		**2**	
	100 K	230 K	100 K	230 K
$d(Fe-N)_{av}$	2.057(4)	2.183(3)	2.034(3)	2.182(3)
V_{UC} [Å^3]	9781(7)	10058(2)	9829(5)	10023(1)
δ(A)	−1.22	−0.74	−1.13	−0.74
δ(B)	−0.39	−0.63	−0.43	−0.63

At 230 K, the crystal packing of the $TCNQ^{\bullet\delta-}$ anions in **1** is quite regular. The two crystallographically unique anions pack in the sequence ABBABB… along the *b* axis, with the corresponding interplanar separations being 3.25–3.30–3.25–3.25–3.30 Å (italic labels in Figure 3; the error in the distances is less than 0.01 Å). When the temperature is lowered, the SCO at the Fe^{II} centers causes the decrease in the Fe–N bond lengths. The associated shrinkage of the unit cell is transmitted to the TCNQ substructure in a non-uniform way: the B···B separations remain the same, 3.30 Å, while the A···B separations decrease to 3.19 Å (regular labels in Figure 3). Similar temperature-dependent structural changes are also observed in **2** (Supporting Information, Figure S1).

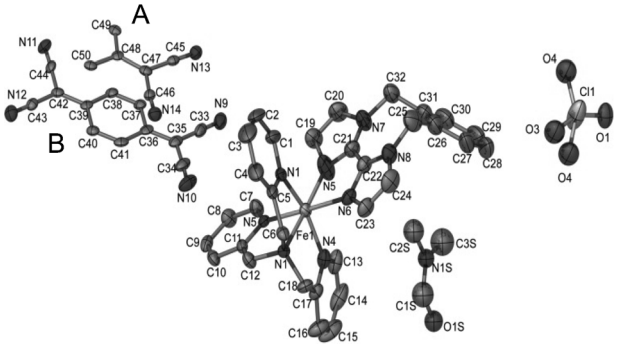

Figure 1. Asymmetric unit of **1**. H atoms are omitted for clarity; ellipsoids are set at 50% probability.

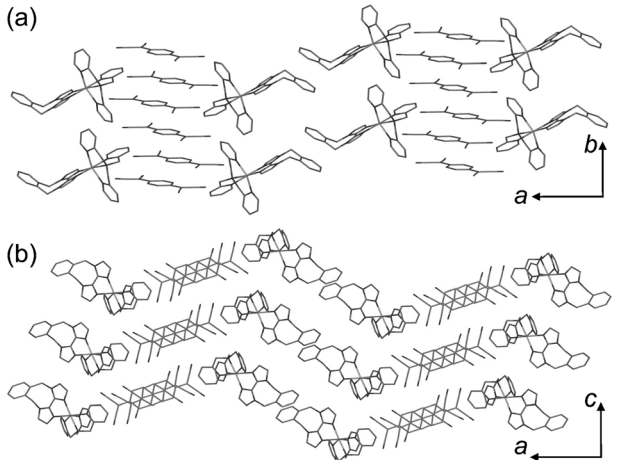

Figure 2. A view of the crystal packing of **1** along the a) *c* and b) *b* axes. H atoms, ClO_4^- anions, and DMF molecules are omitted for clarity.

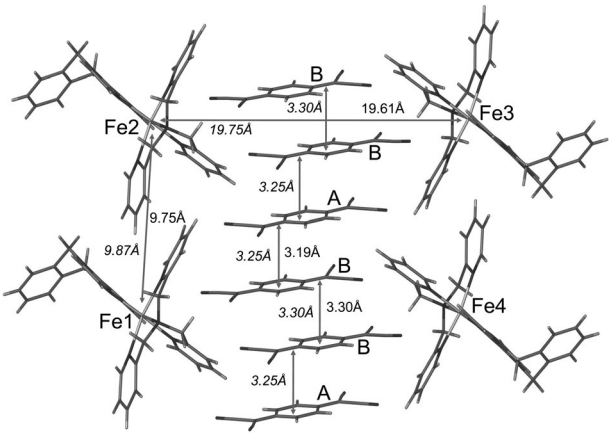

Figure 3. A side view of the crystal packing of **1** with interatomic distances at 230 K and 100 K indicated with italic and regular fonts, respectively. The error in the distances is less than 0.01 Å.

It is well-established that the structures containing the stacks of organic radicals have potential to exhibit significant conductivity if the radical carries a non-integer charge.[10] Based on the formulas of **1** and **2**, the average charge on the $TCNQ^{\bullet\delta-}$ radical should be −0.67, or −2.0 per the repeat ABB unit of the stack. It was shown, however, that the oxidation state of TCNQ is well-reflected by its bond distances. Given the presence of two non-equivalent radicals in the structure, we used the Kistenmacher relationship, $\delta = -41.67[c/(b+$

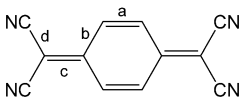

Scheme 1. Metric parameters used in the Kistenmacher equation.

d)] + 19.83, to estimate the charge distribution in the TCNQ stack (Scheme 1).[12]

In **1**, the charges on the radicals A and B are nearly equal at 230 K (−0.51 and −0.43, respectively). As the Kistenmacher relationship was derived for the structures established at room temperature, we scaled the calculated values to make the total charge equal to −1 per 1.5 TCNQ units, that is, to maintain the electroneutrality of the structure (Table 2). Thus, in **1** at 230 K, the charges on TCNQ radicals become −0.74 for A and −0.63 for B, for a ratio of $\delta(A)/\delta(B) = 1.17$. Upon cooling to 100 K, the temperature at which the majority of Fe^{II} centers are LS, the charges become −1.22 and −0.39, respectively, with $\delta(A)/\delta(B) = 3.13$. Similar changes to the charge distribution are also observed in **2** (Supporting Information, Table S3). The more uniform charge distribution in the HS structure correlates well with the more regular interplanar spacing between the TCNQ units and suggests that electrons are more delocalized in the HS state.

Complexes **1** and **2** exhibit the room-temperature χT values of 3.25 and 3.24 emu K mol^{-1}, respectively, which are typical for the HS state of the Fe^{II} ion ($S = 2$). The slight increase from the theoretically expected spin-only value of 3.00 emu K mol^{-1} is explained by a small orbital contribution.[11,13] Upon cooling, the χT values of both complexes decrease in the range from 200 to 100 K (Figure 4a), confirming a gradual temperature-induced SCO. The anion has a little impact on the character and temperature of the SCO, with the midpoint of the transition being observed at $T_{1/2} = 145$ K for **1** and $T_{1/2} = 160$ K for **2**.

The light-induced excited spin state trapping (LIESST) effect was also studied on sample **1**. The complex was irradiated in the SQUID chamber by a 445 nm laser (15 mW cm^{-2}) at 5 K, under a constant magnetic field of 0.1 T. Upon irradiation, the magnetic susceptibility increased significantly and saturated after three hours of irradiation. The comparison of the χT product of the photoinduced state to that of the HS state at 250 K indicated a quantitative light-induced LS→HS conversion in complex **1** at low temperature (Figure 4b).

After the laser was turned off, the sample was warmed up from 5 to 25 K at 3 K min^{-1}, from 25 to 80 at 0.3 K min^{-1}, and from 80 to 25 K at 3 K min^{-1}. The initial slight increase in χT is associated with the zero-field splitting effects. In the range of 40–60 K, an abrupt decrease in the χT value was observed, indicating the thermally activated HS→LS relaxation, which was complete at 65 K. The relaxation temperature, $T_{LIESST} = 50$ K, was found as the minimum in $\partial(\chi T)/\partial T$. As the temperature was increased further, the thermally induced LS→HS conversion was observed, and the curve obtained upon warming essentially matched the one obtained upon cooling.

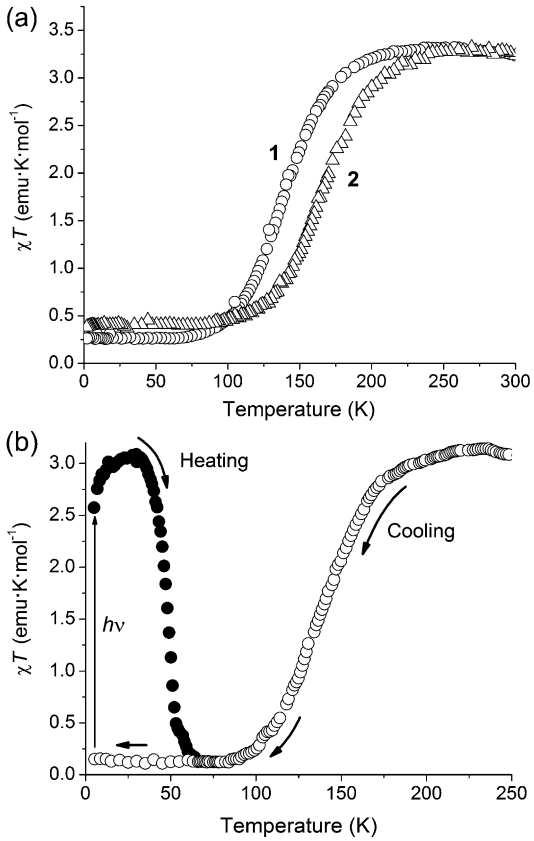

Figure 4. a) Temperature dependence of χT for **1** (○) and **2** (△) measured in the cooling mode. b) Temperature dependence of χT for **1** measured in the cooling mode (○) and then in the warming mode after irradiation with the 445 nm laser at 5 K (●).

The conductivity measurements were performed on a single crystal of **1** along the *b* axis, which coincides with the direction of the TCNQ stack. The value of conductivity at room temperature appeared to be sensitive to the procedure used to prepare electrical contacts, but the average value of 0.2 S cm^{-1} falls in a reasonable range for this class of materials (Table 1). In particular, we note that even higher conductivity was reported by Dunbar et al. for a structurally similar stack of TCNQ radicals co-crystallized with a paramagnetic Mn^{II} complex.[14] As the temperature is lowered, the conductivity of **1** decreases, indicating semiconducting behavior. The activation energy (E_a) estimated from the $\ln(R/R_0)$ vs. $1/T$ plot is equal to 110 meV (Figure 5). The E_a value gradually becomes substantially lower (10 meV) in the low-temperature region. Such behavior might be caused by the closer approach of the TCNQ units, which should increase the band dispersion. Indeed, the change in the E_a takes place in the 100–125 K temperature range, which coincides with the completion of the HS→LS conversion in **1**. A change in the activation energy above and below the SCO region was also reported by Oshio et al.[7c] for $[Fe(dppTTF)_2][Ni(mnt)_2]_2$-$(BF_4)$·PhCN (dppTTF = 1-{2-(1,3-dithiol-2-ylinene)-1,3-dithiolyl}-2-{2,6-bis(1-pyrazolyl)pyridyl}-ethylene, mnt = maleonitriledithiolate), but the difference in the E_a values was smaller: 129 meV in the LS state vs. 119 meV in the HS state.

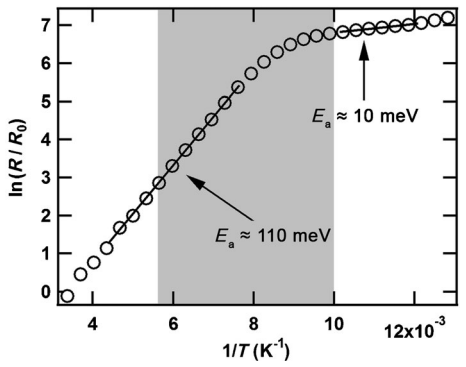

Figure 5. Dependence of the relative resistance of sample **1** on the inverse temperature. Two regions of distinctly different activation regimes are shown with black linear fits, and the corresponding activation energies are indicated. The shaded area indicates the temperature range of the SCO.

In summary, we prepared two materials that combine cationic spin-crossover complexes with partially charged $TCNQ^{\bullet\delta-}$ radical anions. Both compounds exhibit temperature- and light-induced conversion between the HS and LS states of the Fe^{II} ion, as well as semiconductivity propagated by the TCNQ stacks. To the best of our knowledge, this is the first case of the structurally characterized SCO semiconductors that utilize the $TCNQ^{\bullet\delta-}$ radical and exhibit high electrical conductivity. Furthermore, complexes **1** and **2** exhibit the LIESST effect and thus are rare examples of photoswitchable SCO semiconductors, with only two other cases having been reported.[8d,e] The measurements on the changes in the conductivity associated with the light-induced LS→HS conversion are still missing in all the known cases. Our current efforts are directed at implementing such measurements, and their results will be reported in due course.

Experimental Section

All reactions were performed in an N_2-filled glove box. TCNQ (7,7′,8,8′-tetracyanoquinodimethane) was obtained from TCI and all other reagents and anhydrous solvents were obtained from Aldrich and used as received. Ligands tpma (tris(2-pyridylmethyl)amine),[15] xbim (1,1′-(α,α′-*o*-xylyl)-2,2′-bisimidazole),[16] and $(Bu_4N)TCNQ$[17] were synthesized according to the published procedures.

Caution! The complexes between metal ions and organic ligands with perchlorate anions are potentially explosive. The compounds should be prepared in small amounts and handled with great care!

$[Fe(tpma)(xbim)](ClO_4)(TCNQ)_{1.5}\cdot DMF$ (**1**): $Fe(ClO_4)_2\cdot 6H_2O$ (18.1 mg, 0.05 mmol), tpma (14.5 mg, 0.05 mmol), and xbim (11.8 mg, 0.05 mmol) were dissolved in a mixture of DMF (0.8 mL) and acetone (2.0 mL). The obtained yellow–orange solution was added to a mixture of TCNQ (10.2 mg, 0.05 mmol) and $(Bu_4N)TCNQ$ (22.3 mg, 0.05 mmol). The vial with the resulting solution was placed inside a larger vial, the bottom of which was filled with Et_2O for slow vapor diffusion. Large black shiny plate crystals of **1** formed after a few days. They were collected and washed with Et_2O. Yield = 43.6 mg (75%). IR (CN): $\tilde{\nu}$ = 2196, 2175, 2161, 2155 cm^{-1}. Elemental analysis calcd. (%) for **1**·0.5 DMF ($FeClO_{5.5}C_{54.5}N_{15.5}H_{46.5}$): C 59.62, H 4.27, N 19.78; found: C 59.29, H 4.20, N 19.56.

$[Fe(tpma)(xbim)](BF_4)(TCNQ)_{1.5}\cdot DMF$ (**2**): Compound **2** was prepared in a manner analogous to that described for **1**, using $Fe(BF_4)_2\cdot 6H_2O$ (16.9 mg, 0.05 mmol), tpma (14.5 mg, 0.05 mmol), DMF (0.7 mL), and acetone (2.0 mL). Black shiny thin plate crystals that formed after a few days were collected and washed with Et_2O. Yield = 28.9 mg (50%). IR (CN): $\tilde{\nu}$ = 2197, 2175, 2161, 2156 cm^{-1}. Elemental analysis calcd. (%) for **1**·0.5 DMF ($FeBF_4O_{1.5}C_{54.5}N_{15.5}H_{46.5}$): C 60.32, H 4.32, N 20.01; found: C 60.11, H 4.18, N 19.78.

Electrical transport was measured on a single crystal of **1** along the *b* axis by the 4-probe DC method (Keithley 6221 and 6517A) using carbon paste electrodes. The proper orientation was established by face-indexing of the crystal by means of X-ray diffraction. At least a dozen transport measurements have been performed in various sample configurations. It was noted that the sample was unusually brittle around the SCO region at about 145 K. To minimize the stress/strain on the sample, soft gold-coated spider silk fibers with a diameter of about 4 μm were eventually used as electrical wires to achieve reliable temperature-dependent data.[18]

Received: September 1, 2014
Published online: November 21, 2014

Keywords: conductivity · iron · semiconductors · spin crossover · TCNQ

[1] E. Coronado, J. R. Galán-Mascarós, C. J. Gomez-García, V. Laukhin, *Nature* **2000**, *408*, 447–449.
[2] a) E. Coronado, P. Day, *Chem. Rev.* **2004**, *104*, 5419–5448; b) E. Coronado, J. R. Galán-Mascarós, *J. Mater. Chem.* **2005**, *15*, 66–74; c) P. Dechambenoit, J. R. Long, *Chem. Soc. Rev.* **2011**, *40*, 3249–3265; d) J. R. Galán-Mascarós, E. Coronado, P. A. Goddard, J. Singleton, A. I. Coldea, J. D. Wallis, S. J. Coles, A. Alberola, *J. Am. Chem. Soc.* **2010**, *132*, 9271–9273.
[3] E. Coronado, J. R. Galán-Mascarós, C. J. Gomez-García, E. Martinez-Ferrero, S. van Smaalen, *Inorg. Chem.* **2004**, *43*, 4808–4810.
[4] a) D. Gatteschi, R. Sessoli, J. Villain, *Molecular Nanomagnets*, Oxford University Press, New York, **2006**; b) R. Bagai, G. Christou, *Chem. Soc. Rev.* **2009**, *38*, 1011–1026.
[5] a) P. Gütlich, H. A. Goodwin, *Top. Curr. Chem.* **2004**, *233*, 1–47; b) K. S. Murray in *Spin-Crossover Materials*: *Properties and Applications* (Ed.: M. A. Halcrow), Wiley, New York, **2013**, pp. 1–54.
[6] a) A. Hauser, *Top. Curr. Chem.* **2004**, *233*, 49–58; b) A. Hauser, *Top. Curr. Chem.* **2004**, *234*, 155–198.
[7] a) A. B. Gaspar, V. Ksenofontov, M. Seredyuk, P. Gütlich, *Coord. Chem. Rev.* **2005**, *249*, 2661–2676; b) O. Sato, Z.-Y. Li, Z.-S. Yao, S. Kang, S. Kanegawa in *Spin-Crossover Materials*: *Properties and Applications* (Ed.: M. A. Halcrow), Wiley, New York, **2013**, pp. 303–319; c) M. Nihei, N. Takahashi, H. Nishikawa, H. Oshio, *Dalton Trans.* **2011**, *40*, 2154–2156.
[8] a) S. Dorbes, L. Valade, J. A. Real, C. Faulmann, *Chem. Commun.* **2005**, 69–71; b) C. Faulmann, S. Dorbes, B. G. de Bonneval, G. Molnar, A. Bousseksou, C. J. Gomez-Garcia, E. Coronado, L. Valade, *Eur. J. Inorg. Chem.* **2005**, 3261–3270; c) C. Faulmann, K. Jacob, S. Dorbes, S. Lampert, I. Malfant, M. L. Doublet, L. Valade, J. A. Real, *Inorg. Chem.* **2007**, *46*, 8548–8559; d) K. Takahashi, H. B. Cui, Y. Okano, H. Kobayashi, H. Mori, H. Tajima, Y. Einaga, O. Sato, *J. Am. Chem. Soc.* **2008**, *130*, 6688–6689; e) K. Takahashi, H. B. Cui, Y. Okano, H. Kobayashi, Y. Einaga, O. Sato, *Inorg. Chem.* **2006**, *45*, 5739–5741; f) K. Fukuroi, K. Takahashi, T. Mochida, T. Sakurai, H. Ohta, T. Yamamoto, Y. Einaga, H. Mori, *Angew. Chem. Int. Ed.* **2014**, *53*, 1983–1986; *Angew. Chem.* **2014**, *126*, 2014–2017.

[9] P. J. Kunkeler, P. J. van Koningsbruggen, J. P. Cornelissen, A. N. van der Horst, A. M. van der Kraan, A. L. Spek, J. G. Haasnoot, J. Reedijk, *J. Am. Chem. Soc.* **1996**, *118*, 2190 – 2197.
[10] T. Mori, *Chem. Rev.* **2004**, *104*, 4947 – 4969.
[11] H. V. Phan, P. Chakraborty, M. M. Chen, Y. M. Calm, K. Kovnir, L. K. Keniley, J. M. Hoyt, E. S. Knowles, C. Besnard, M. W. Meisel, A. Hauser, C. Achim, M. Shatruk, *Chem. Eur. J.* **2012**, *18*, 15805 – 15815.
[12] T. J. Kistenmacher, T. J. Emge, A. N. Bloch, D. O. Cowan, *Acta Crystallogr. Sect. B* **1982**, *38*, 1193 – 1199.
[13] a) R. L. Carlin, *Magnetochemistry*, Springer, Berlin, **1986**; b) M. Shatruk, A. Dragulescu-Andrasi, K. E. Chambers, S. A. Stoian, E. L. Bominaar, C. Achim, K. R. Dunbar, *J. Am. Chem. Soc.* **2007**, *129*, 6104 – 6116.
[14] M. Ballesteros-Rivas, A. Ota, E. Reinheimer, A. Prosvirin, J. Valdes-Martinez, K. R. Dunbar, *Angew. Chem. Int. Ed.* **2011**, *50*, 9703 – 9707; *Angew. Chem.* **2011**, *123*, 9877 – 9881.
[15] T. Kojima, R. A. Leising, S. Yan, L. Que, Jr., *J. Am. Chem. Soc.* **1993**, *115*, 11328 – 11335.
[16] R. P. Thummel, V. Goulle, B. Chen, *J. Org. Chem.* **1989**, *54*, 3057 – 3061.
[17] L. R. Melby, R. J. Harder, W. R. Hertler, W. Mahler, R. E. Benson, W. E. Mochel, *J. Am. Chem. Soc.* **1962**, *84*, 3374 – 3387.
[18] E. Steven, J. G. Park, A. Paravastu, E. B. Lopes, J. S. Brooks, O. Englander, T. Siegrist, P. Kaner, R. G. Alamo, *Sci. Technol. Adv. Mater.* **2011**, *12*, 055002.
[19] CCDC 1009090 (**1**) and CCDC 1009091 (**2**) contain the supplementary crystallographic data for this paper. These data can be obtained free of charge from The Cambridge Crystallographic Data Centre via www.ccdc.cam.ac.uk/data_request/cif.

